Optimum Parking Orbit Orientation for a Three-Dimensional Capture-Escape Mission

D. E. CORNICK* AND L. K. SEVERSIKE†
Iowa State University, Ames, Iowa

The capture and escape maneuvers required to establish a stopover orbit around a planet for a given interplanetary mission can be expensive in terms of total mission fuel requirements. An analytical and computational technique to determine the optimum orientation of the stopover orbit (longitude of the ascending node, orbit periapsis location, and the positions of the capture and escape maneuvers) such that the total velocity increment required for the two impulsive maneuvers is a minimum, is presented. Davidon's method, using a finite differencing technique to calculate the gradient vector, is employed in the optimization process. This approximation to the gradient vector proved to be sufficiently accurate to permit convergence to a solution. The technique has been programmed for a digital computer so that parametric studies can be made for arbitrary stopover orbits and planetary missions. Results are presented for a 1973 Mars mission and a 1978 Venus mission.

Nomenclature

$\hat{A}$ = unit vector toward ascending node
a = semimajor axis of conic section
C_3 = vis-viva energy integral
e = eccentricity of conic section
h = magnitude of specific angular momentum
i = inclination of stopover orbit
JD = Julian date
$\hat{k}$ = unit vector along positive z axis
K_2, K_4 = quantities defined in Eq. (8)
n = apsidal ratio (r_a/r_p) of stopover orbit
p = semi latus rectum
$\bar{r}$ = position vector at injection point
$\hat{r}$ = unit position vector at injection point
r = magnitude of position vector
r_a = apoapsis radius
r_p = periapsis radius
$\hat{S}$ = unit vector in direction of hyperbolic asymptote
t = time parameter
$\bar{V}$ = velocity vector at injection point
$\hat{V}$ = unit velocity vector at injection point
V = magnitude of velocity vector
$\bar{V}_p$ = target planet's velocity vector
$\bar{V}_\infty$ = hyperbolic excess velocity vector
$\Delta\bar{V}$ = velocity increment vector for injection maneuver
ΔV = magnitude of velocity increment vector
$\hat{W}_h$ = unit vector in direction of angular momentum vector of hyperbola
α = right ascension of hyperbolic asymptote
β = angle between injection position vector $\bar{r}$ and hyperbolic asymptote $\hat{S}$
γ = flight path angle at injection point
δ = declination of hyperbolic asymptote
θ = true anomaly of injection point in stopover orbit
μ = gravitational constant for central body
ρ = angle between ascending node and injection point in stopover orbit
ρ_a = angle between stopover ascending node and projection of hyperbolic asymptote onto stopover orbit plane
σ = nondimensional ratio, $C_3 r/2\mu$
τ = mean orbital motion
ϕ = true anomaly of injection point in hyperbola
ϕ_a = true anomaly of hyperbolic asymptote in hyperbola
ω = argument of periapsis of stopover orbit
$\dot{\omega}$ = time rate of change of argument of periapsis
Ω = right ascension of ascending node of stopover orbit
$\dot{\Omega}$ = time rate of change of right ascension of ascending node
$\hat{\zeta}$ = unit vector in direction of angular momentum vector of stopover orbit
$[\ ]_k$ = rotation matrix about a k axis
xyz = planet equatorial reference frame
$\xi\eta\zeta$ = stopover orbit reference frame with ξ axis in the direction of the ascending node

Subscripts

$(\ )_C$ = refers to capture hyperbola quantity
$(\ )_e$ = refers to escape hyperbola quantity
$(\ )_h$ = refers to hyperbola quantity

Received August 18, 1969; presented as Paper 69-918 at the AIAA/AAS Astrodynamics Conference, Princeton, N.J., August 20–22, 1969; revision received March 9, 1970. The authors gratefully appreciate the assistance from A. C. Young and R. Ellison of Marshall Space Flight Center, Huntsville, Ala., and the financial assistance provided by the Iowa State University Engineering Research Institute, Ames, Iowa.

* Graduate Student, Aerospace Engineering.
† Assistant Professor, Aerospace Engineering. Member AIAA.

Introduction

PLANNING for future manned and unmanned lunar and interplanetary missions requires extensive studies of the possible spacecraft trajectories. Many of these scientific exploration missions will include in their flight profiles a stopover or parking orbit about the target planet.

The establishment of the stopover orbit about the target planet necessitates a velocity increment to reduce the spacecraft's velocity along the incoming hyperbolic path to the proper velocity required to go into the parking orbit. After a certain stay-time in the stopover orbit, determined by mission objectives, another velocity increment is required to permit the spacecraft to escape from the target planet along an outgoing hyperbolic path that is the beginning of the return leg to the Earth. A schematic of the mission showing the heliocentric and planetocentric phases is presented in Figs. 1 and 2.

Ideally the approach hyperbolic asymptote and the stopover orbit would lie in the same plane so that an inplane capture maneuver could be performed. Coplanar geometry conditions for the departure hyperbolic asymptote and the stopover orbit are also desirable. In general, however, this coplanar relationship will not be satisfied because of the dynamic nature of the relative geometry of the asymptotes and the parking orbit. The orientation of the approach and departure asymptotes is a function of time as is the orientation of the stopover orbit due to the perturbations resulting

from the planet's oblateness. Hence, a coplanar transfer can be accomplished at only one time when the hyperbolic asymptote and the orbit plane are contained in the same plane. For this case, the optimum injection position is at the periapsis of the hyperbola. If the parking orbit is elliptical, then this point should coincide with the periapsis of the ellipse for the optimum single impulse injection. Since this coplanar injection is very restrictive from a mission planning standpoint, a noncoplanar maneuver is more realistic. The optimum position for the noncoplanar transfer will not necessarily occur at the periapsis of the parking orbit so that a ΔV penalty will result due to both the plane change maneuver and the path angle change. Since these ΔV penalties can become large, it is desirable to minimize this effect. Although these two velocity impulses, one for the capture maneuver and one for the escape maneuver, constitute only a portion of the total velocity increment requirements for the entire mission, they can represent a considerable percentage of the total, especially for missions to the more massive planets. As a consequence, minimization of the total velocity increment necessary for the capture and escape maneuvers can produce a significant reduction in the total mission fuel requirements. Therefore, it is desirable to determine the orientation of the stopover orbit and the capture and escape injection positions that will minimize the velocity increments. This problem is called the stopover orbit launch window problem.

The coplanar stopover orbit launch window problem has been examined for the optimum orientation of the parking orbit excluding the effects of the planet's oblateness in Refs. 1 and 2. In Ref. 3, the analytical considerations for the general three-dimensional launch window problem have been treated. The planar finite thrust transfer between planet approach and departure asymptotes with a specified intermediate orbit was evaluated in Ref. 4. Several other papers have considered either the optimum capture or escape problem, but not the combination of these two modes.[5,6]

This paper analyzes a technique for determining the optimum parking orbit orientation for the three-dimensional stopover orbit launch window problem. Davidon's method is used to minimize the total velocity increment with respect to the four variables, the longitude of the ascending node, the periapsis location of the stopover orbit, and the position of the injection points for the capture and escape maneuvers. The parking orbit is assumed to be elliptical and is, in general, not coplanar with either the approach or the departure hyperbolic asymptotes. Only two velocity impulses are considered, one for capture and one for escape from the stopover orbit. Perturbations of the parking orbit due to the target

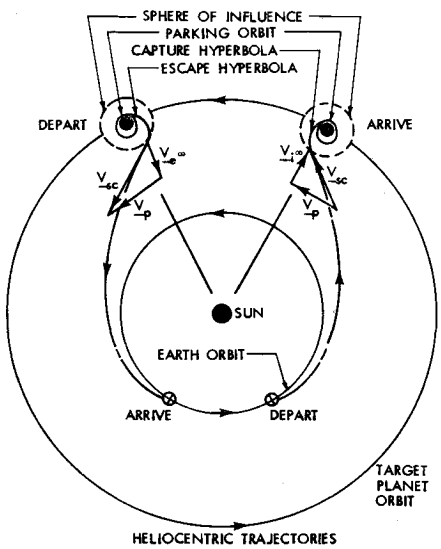

Fig. 1 Heliocentric trajectory phase.

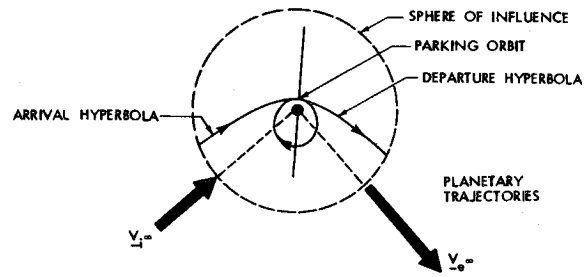

Fig. 2 Planetocentric trajectory phase.

planet's oblateness are included. The gradient of the performance functional is approximated by differencing and it is shown that this approximation does not, in this case, prevent convergence. Along with the analytical considerations involved, a description of the digital computer program is included. The results of this study indicate that deflected gradient schemes can be utilized very effectively for this type of launch window problem.

Analytical Development

The analytical technique for calculating the velocity increment functional to be minimized is developed for the three-dimensional capture-escape launch window problem. Capture into an elliptical parking orbit about the target planet is accomplished by applying a velocity impulse at the intersection of the approach hyperbolic trajectory and the stopover orbit. After a certain stay time during which the orbit orientation will have changed due to the planet's oblateness, a second velocity impulse is applied at the point where the stopover orbit and the departure hyperbolic trajectory intersect. The total velocity increment is then optimized yielding the optimum orientation of the parking orbit and the injection conditions (velocity and position vectors) for a specified interplanetary mission and stopover orbit.

The development is based upon the following assumptions: 1) the spacecraft is treated as a point mass and two-body mechanics are used for the capture hyperbola, elliptical stopover orbit, and the escape hyperbola; 2) the general elliptical parking orbit may have any orientation, and its motion is due to the nodal regression and the advance of the periapsis due to the perturbations caused by the oblateness of the planet; 3) the orientation of the approach hyperbolic asymptote and the arrival energy are functions of time depending upon the arrival time and the trip-time along the outbound Earth leg of the mission; 4) the orientation of the departure hyperbolic asymptote and the departure energy are functions of time depending upon the departure time and the trip-time along the return Earth leg of the mission; 5) the capture and escape maneuvers are accomplished by a single impulsive velocity change, thereby resulting in a total of two-impulsive

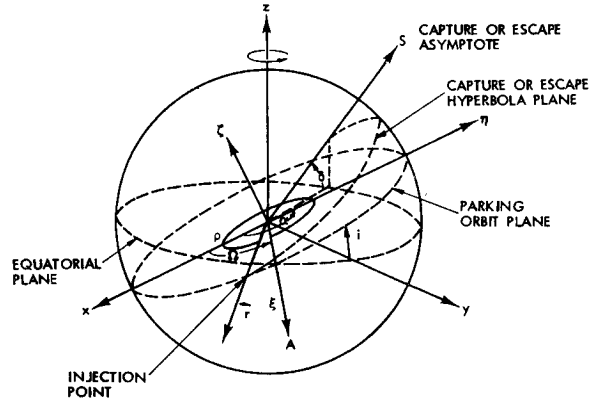

Fig. 3 Noncoplanar stopover orbit launch window geometry.

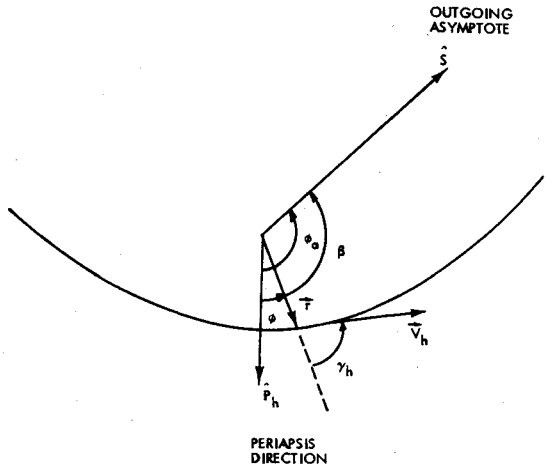

Fig. 4 Inplane escape hyperbola geometry.

velocity increments; and 6) the stay time in the parking orbit around the target planet is limited to a fraction of the planet's orbital period.

Figure 3 shows the basic geometry for the noncoplanar launch problem. The inertial xyz axes system is oriented such that the x axis points toward the vernal equinox and the z axis is normal to the equatorial plane. The orthogonal $\xi\eta\zeta$ axes system has the ξ axis in the stopover orbit plane along the line of the ascending node and the ζ axis normal to the parking orbit plane along the angular momentum vector. The inplane geometry for the escape hyperbola is presented in Fig. 4.

The impulsive velocity increment required for either the capture or the escape maneuver can be expressed as a function of the energy level C_3, the right ascension α and declination δ of the hyperbolic asymptote vector $\hat{S}$, the parking orbit inclination i, the semimajor axis a, the orbit eccentricity e, the argument of periapsis ω, the right ascension Ω of the ascending node of the parking orbit, and the injection location ρ in the parking orbit. Hence, the functional form for the velocity increment for a vehicle to transfer from a heliocentric conic to a planetocentric parking orbit is

$$\Delta\bar{V}_C = \Delta\bar{V}_C[C_3(t),\alpha(t),\delta(t),i,a,e,\omega(t),\Omega(t),\rho_C] \quad (1)$$

As noted, the energy level and the hyperbolic asymptote are functions of time as are the orientation angles of the parking orbit. Hence, these parameters must be evaluated at the time of capture.

The similar expression for the escape velocity increment from the parking orbit to the heliocentric conic is given in functional form as

$$\Delta\bar{V}_e = \Delta\bar{V}_e[C_3(t),\alpha(t),\delta(t),i,a,e,\omega(t),\Omega(t),\rho_e] \quad (2)$$

where the parameters must be evaluated at the time of escape.

The sum of the two impulses is the function that is to be optimized

$$\Delta V_{\text{total}} = |\Delta\bar{V}_C| + |\Delta\bar{V}_e| \quad (3)$$

For a given mission the orbital parameters a, e, and i will be specified. Depending upon the Earth launch opportunities and the vehicle performance capabilities, the energy level C_3 and the approach asymptote $\hat{S}$ will also be specified. Similarly the energy level and the departure asymptote will be specified depending upon mission objectives and system capabilities.

The motion of the stopover orbit relative to the planet during the stopover is accounted for by the secular perturbations due to the planet's oblateness as

$$\Omega_e = \Omega_C + \dot{\Omega}(\text{JD}_e - \text{JD}_C) \quad (4)$$

$$\omega_e = \omega_C + \dot{\omega}(\text{JD}_e - \text{JD}_C) \quad (5)$$

where $\dot{\Omega}$ and $\dot{\omega}$ depend upon the parking orbit size, shape, and inclination and the physical properties of the target planet, e.g., mass and the second harmonic coefficient J_2. For Mars

$$\dot{\Omega} = -\tau\cos i[3(K_2/p^2) + 10(K_2/p^4)(1 + 1.5e^2) \times (1 - 1.75\sin^2 i)] \quad (6)$$

$$\dot{\omega} = \tau\,[3(K_2/p^2)(1 - 1.5\sin^2 i) + 10\,(K_4/p^4) \times (1 + 0.75e^2)(1 - 5\sin^2 i + 4.375\sin^4 i)] - \dot{\Omega}\cos i \quad (7)$$

where

$$p = a(1 - e^2),\ K_2 = 7.03656 \times 10^5/\tau^2$$
$$K_4 = 2.2517 \times 10^6/\tau^2,\ \tau = [\mu/a^3]^{1/2} \quad (8)$$

For short stay times or for a planet such as Venus, $\dot{\Omega} \cong 0$ and $\dot{\omega} \cong 0$.

Therefore, for a specified stopover time, the optimum orbit orientation angles, Ω_e and ω_e, can be calculated for the corresponding optimum conditions at the capture time. Hence, the parameters Ω and ω appearing in Eqs. (1) and (2) are related.

As a result, Eq. (3) may be rewritten as

$$\Delta v_{\text{total}} = \Delta v(\omega,\Omega,\rho_C,\rho_e) \quad (9)$$

or as a function of the four independent variables; the longitude of the ascending node, the periapsis of the parking orbit, and the location of the injection points for the capture and escape maneuvers.

Basically there are three phases to the calculation of the performance functional; 1) stopover capture orbit conditions, 2) injection conditions for both the capture and escape maneuvers, and 3) computation of the total velocity increment.

Stopover Capture Orbit Conditions

The stopover orbit about the target planet is specified by the parameters a, e, and i or alternatively by r_p, n, and i where

$$r_p = a(1 - e) \quad (10)$$

$$n = r_a/r_p = (1 + e)/(1 - e) \quad (11)$$

The orientation angles Ω and ω for both the capture time and escape time are to be determined for the optimum conditions.

Since the $\xi\eta$-plane lies in the orbit plane, the unit vector along the line of ascending nodes can be expressed as $\hat{A} = (1,0,0)$ or, in the xyz system,

$$\hat{A} = [-\Omega]_3[-i]_1\begin{bmatrix}1\\0\\0\end{bmatrix} \quad (12)$$

where the rotation matrix $[-\theta_1]_K$ indicates the inverse of the rotation matrix $[\theta_1]_K$ with argument θ_1 about the K axis. The injection position vector in the equatorial reference frame is

$$\bar{r} = r\hat{r} \quad (13)$$

where

$$r = a(1 - e^2)/(1 + e\cos\theta) \quad (14)$$

and

$$\hat{r} = [-\Omega]_3[-i]_1[-\rho]_3\begin{bmatrix}1\\0\\0\end{bmatrix} \quad (15)$$

Now the true anomaly θ measured in the orbit plane is

$$\theta = \chi + \rho = 2\pi + \rho - \omega \tag{16}$$

The velocity vector in the same reference frame is given by

$$\bar{V} = V\hat{V} \tag{17}$$

where

$$V^2 = \mu[(2/r) - (1/a)] \tag{18}$$

Since the flight path angle γ is the angle between the radial direction and the velocity vector, then the unit velocity vector is

$$\hat{V} = [-\Omega]_3[-i]_1[-\rho]_3[-\gamma]_3\begin{bmatrix}1\\0\\0\end{bmatrix} \tag{19}$$

The flight path angle can be determined from angular momentum considerations

$$\bar{h} = \bar{r} \times \bar{V} = rV \sin\gamma\hat{\zeta} = h\hat{\zeta} \tag{20}$$

Since

$$h = [\mu a(1 - e^2)]^{1/2} \tag{21}$$

then

$$\gamma = \sin^{-1}\{[\mu a(1 - e^2)]^{1/2}/rV\} \tag{22}$$

where

$$0 \leqq \gamma \leqq \pi/2 \text{ for } 0 \leqq (\rho - \omega) \leqq \pi$$

and

$$\pi/2 < \gamma < \pi \text{ for } \pi < (\rho - \omega) < 2\pi$$

Capture and Escape Injection Conditions

The conditions for the planetocentric capture or escape hyperbolic trajectories can be calculated in the following manner. For the specified Julian date JD_C or JD_e, for the capture or escape maneuver, the injection conditions (α,δ,C_3) are predetermined. Hence, the unit vector in the direction of the incoming or outgoing hyperbolic asymptote is

$$\hat{S} = [-\alpha]_3[\delta]_2\begin{bmatrix}1\\0\\0\end{bmatrix} \tag{23}$$

The injection position vector (magnitude and direction) is given by Eqs. (13–15). In terms of the hyperbolic parameters

$$r = a_h(e_h^2 - 1)/(1 + e_h \cos\phi) \tag{24}$$

where the inplane geometry for the hyperbolic trajectory is shown in Fig. 4.

The velocity vector $\bar{V}_h$ in the planet's equatorial reference frame is

$$\bar{V}_h = V_h\hat{V}_h \tag{25}$$

where

$$\hat{V}_h = \hat{r}\cos\gamma_h + (\hat{W}_h \times \hat{r})\sin\gamma_h \tag{26}$$

and

$$V_h^2 = \mu[(2/r) + (1/a_h)] \tag{27}$$

Now, since the energy level C_3 is known and defined as

$$C_3 = \mu/a_h = V_\infty^2 \tag{28}$$

the magnitude of the velocity vector becomes

$$V_h^2 = (2\mu/r) + C_3 \tag{29}$$

Again use the angular momentum concept to determine the flight-path angle between the radial direction and the velocity vector

$$\bar{h}_h = \bar{r} \times \bar{V}_h = rV_h \sin\gamma_h\hat{W}_h = h_h\hat{W}_h \tag{30}$$

Since

$$h_h = [a_h\mu(e_h^2 - 1)]^{1/2} = \mu[(e_h^2 - 1)/C_3]^{1/2} \tag{31}$$

then

$$\gamma_h = \sin^{-1}\{\mu[(e_h^2 - 1)/C_3]^{1/2}/rV_h\} \tag{32}$$

The eccentricity can be obtained from the true anomaly of the hyperbolic asymptote ϕ_a since

$$\cos\phi_a = -1/e_h \tag{33}$$

or

$$e_h = (\tan^2\phi_a + 1)^{1/2} \tag{34}$$

From Ref. 6 for an incoming asymptote

$$\tan\phi_a = \sigma\sin\beta + [(1 + \sigma)^2 - (1 - \sigma\cos\beta)^2]^{1/2} \tag{35}$$

and for an outgoing asymptote

$$\tan\phi_a = -\sigma\sin\beta - [(1 + \sigma)^2 - (1 + \sigma\cos\beta)^2]^{1/2} \tag{36}$$

where the dimensionless parameter σ is defined as

$$\sigma = C_3r/2\mu \tag{37}$$

The unit vector hyperbolic angular momentum can be determined as

$$\hat{W}_h = (\hat{r} \times \hat{S})/\sin\beta \tag{38}$$

The determination of the true anomaly ϕ of the injection position vector, the orientation angle ϕ_a of the asymptote, and the angle β are all related and depend upon the orientation of the plane of the hyperbola. Once the orientation of the hyperbolic plane has been established the angle ϕ can be determined, since it is measured in the direction of the motion along the hyperbola. If $\hat{W}_h \cdot \hat{k}$ is positive, then the motion is called direct, and if $\hat{W}_h \cdot \hat{k}$ is negative, the motion is retrograde. The convention that β is positive when measured in the direction of motion along the hyperbola going from $\hat{r}$ to $\hat{S}$ was adopted. Therefore,

$$\beta = \cos^{-1}(\bar{r} \cdot \hat{S}) \tag{39}$$

and

$$\phi = \phi_a - \beta \tag{40}$$

It should be noted that the injection maneuver for either the capture or escape hyperbola can be accomplished on either the incoming or the outgoing leg. Therefore, the flight path angle is dependent upon the angle ϕ. For

$$0 \leqq \phi < \pi,\ 0 < \gamma_h \leqq \pi/2$$

and for

$$\pi < \phi < 2\pi,\ \pi/2 < \gamma_h < \pi$$

It therefore becomes apparent that a considerable amount of logic must be included to assure that the proper geometry is obtained. Experience has shown that the optimum injection maneuver occurs when the direction of motion in the hyperbola is in the same general direction as the motion in the stopover orbit.

Computation of the Total Velocity Increment

Now that the velocity vectors for the capture and escape hyperbolas along with the velocity vector at the injection points in the stopover orbit have been determined, the velocity increments required to perform the capture and escape maneuvers can be evaluated. The velocity increment for

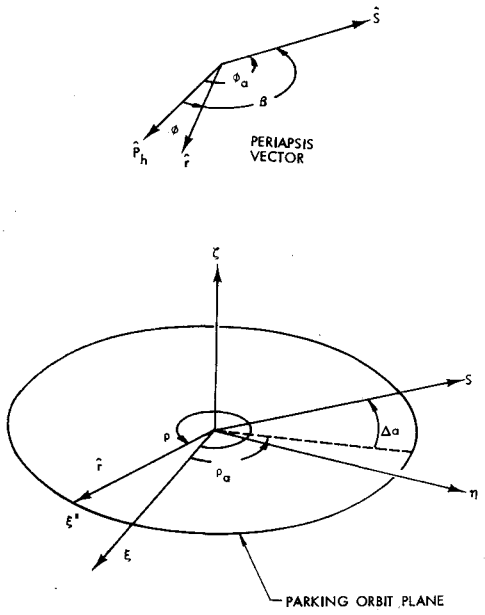

Fig. 5 Relative geometry of hyperbolic asymptote and stopover orbit plane.

capture is

$$\Delta\bar{V}_C = \bar{V}_C - \bar{V}_{hC} \tag{41}$$

or

$$\Delta V_C = |\Delta\bar{V}_C| = [(\bar{V}_C - \bar{V}_{hC}) \cdot (\bar{V}_C - \bar{V}_{hC})]^{1/2} \tag{42}$$

$$\Delta V_C = [V_{hC}^2 + V_C^2 - 2V_C V_{hC}\hat{V}_C \cdot \hat{V}_{hC}]^{1/2} \tag{43}$$

For the escape maneuver the velocity increment is

$$\Delta\bar{V}_e = \bar{V}_{he} - \bar{V}_e \tag{44}$$

or

$$\Delta V_e = [V_{he}^2 + V_e^2 - 2V_e V_{he}\hat{V}_e \cdot \hat{V}_{he}]^{1/2} \tag{45}$$

As a result, the total velocity increment according to Eq. (3) is

$$\Delta V_{\text{total}} = \Delta V_c + \Delta V_e \tag{46}$$

The procedure then is to determine the optimum combination of ω, Ω, ρ_C, and ρ_e such that ΔV_{total} is a minimum for the specified stopover orbit (a,e,i) and the mission parameters (α,δ,C_3) for the capture and escape hyperbolas along with a specified stay-time in the stopover orbit.

Application of Davidon Method

The Davidon method as described in Ref. 7 was selected as the optimization technique for this problem because of the relatively small number of independent variables involved. This version of Davidon's variable metric method requires only function evaluations in the one-dimensional minimization phase, a fact which is particularly significant since the gradient vector is calculated numerically by finite differencing. This approximate gradient information has proven to be accurate enough to enable the Davidon algorithm to converge to a solution. There is a trade-off between the sophistication of the differentiation algorithm and the total computational time. A fourth-order numerical differentiation method that requires four function evaluations per component of the gradient vector was selected. However, since the gradient is only evaluated once each cycle (at the start of each linear minimization), it does not produce a restrictive number of additional function evaluations.

The problem has been programmed for the IBM 360/65 digital computer in Fortran IV language. The solution time is generally less than 10 sec depending strongly upon the convergence tolerances and to a lesser degree upon the initial guess. The input and output information are depicted in Table 1.

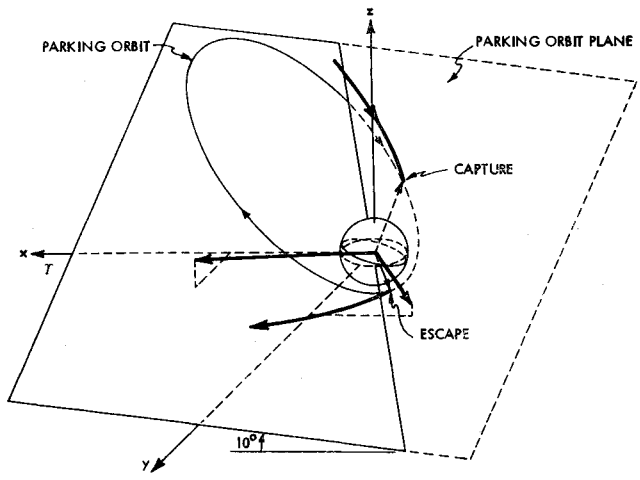

Fig. 6 Mars mission capture-escape geometry.

Numerical Studies

The analytical and computational method described in the previous sections for determining the optimum stopover orbit orientation has been applied to several typical interplanetary missions. The selected missions are only representatives of a more comprehensive parametric study for several classes of missions to the planets Venus and Mars which is currently in progress. A 1978 Venus stopover mission and a 1973 Mars stopover mission were selected for illustration purposes.

1978 Venus Stopover Mission

The incoming asymptote at Venus has a declination of $-31.4°$, a right ascension of 114.4°, and the hyperbolic excess speed is 0.187 EMOS (29.78 km/sec) or 5.56 km/sec (C_3 = 30.88 km²/sec²). After a stay-time the vehicle departs from Venus. The outgoing asymptote has a declination of $-24.7°$, a right ascension of 84.4°, and the hyperbolic excess speed is 0.165 EMOS or 4.91 km/sec (C_3 = 24.14 km²/sec²). The stopover orbit is selected as an ellipse with a = 39,450 km, e = 0.83, and is inclined at 147.91°. The inclination was selected such that the capture and escape maneuvers are

Table 1 Mission parameters[a]

Input parameters: Stopover orbit	Hyperbolas: Capture	Hyperbolas: Escape	Output parameters (Optimum conditions): Capture	Output parameters (Optimum conditions): Escape
a) 1978 Venus mission				
a = 39,450	C_3 = 30.99	24.44	ω = 198.0	198.0
e = 0.8276	α = 114.40	84.84	Ω = 38.12	38.12
i = 147.91	δ = −31.40	24.70	ρ = 268.0	146.0
			ΔV_{total} = 4.1568 km/sec	
b) 1973 unperturbed Mars mission (20-day stay-time)				
a = 19,550	C_3 = 20.6	57.6	ω = 349.75	349.75
e = 0.80	α = 138.0	31.6	Ω = 156.12	156.12
i = 170.0	δ = 5.9	8.9	ρ = 277.29	45.4
			ΔV_{total} = 7.309 km/sec	
c) 1973 perturbed Mars mission (20-day stay-time)				
a = 19,550	C_3 = 20.6	57.6	ω = 322.82	329.99
e = 0.80	α = 138.0	31.6	Ω = 130.76	134.43
i = 170.0	δ = 5.9	8.9	ρ = 248.02	20.06
			ΔV_{total} = 7.284 km/sec	

[a] a is in km; C_3 in km²/sec²; all angles in degrees (see Nomenclature).

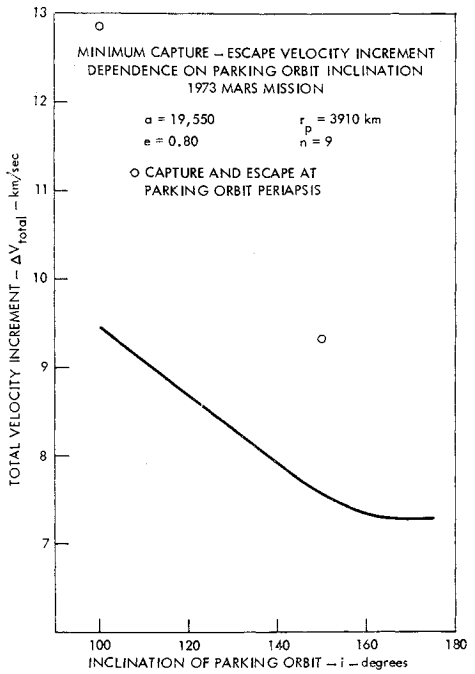

Fig. 7 Optimum total velocity increment dependence on orbit inclination for a 1973 Mars mission.

coplanar with the plane determined by the incoming and outgoing asymptotes. The results for the optimum orientation parameters ω, Ω, ρ_C, ρ_e are shown in Table 1. The corresponding capture and escape maneuver conditions are also shown which yield the minimum total velocity increment of 4.156 km/sec. Note that for Venus $\dot{\omega} = 0$ and $\dot{\Omega} = 0$, so that the stopover orbit has not been perturbed. These results are in good agreement with the results presented in Refs. 1 and 2.

1973 Mars Stopover Mission

A 400 day mission, that departs from Earth in early August 1973, arrives at Mars in early January 1974, goes into an orbit about Mars for a 10 day stay-time, departs from Mars about mid-January 1974, and arrives at Earth about mid-September 1974. The incoming asymptote at Mars has a declination of 5.9°, a right ascension of 138°, and the hyperbolic excess speed is 0.153 EMOS (C_3 = 20.6 km²/sec²). The outgoing asymptote at Mars has a declination of 31.6°, a right ascension of 8.9°, and the hyberbolic excess speed is 0.255 EMOS (C_3 = 57.6 km²/sec²). The stopover orbit has a semimajor axis of 19,550 km and an eccentricity of 0.80. The inclination was selected as 170°. The results for the optimum conditions for the orientation, escape and capture maneuvers, and the minimum total velocity increment are shown in Tables 1b and 1c. The conditions in Table 1b correspond to an unperturbed orbit, i.e., $\dot{\omega} = 0$ and $\dot{\Omega} = 0$, whereas the information presented in Table 1c is for a perturbed orbit. One interesting result that does show up for this case is that the rotation of the periapsis due to the perturbation helps to reduce the total velocity increment since it tends to align the periapsis of the stopover orbit with the escape hyperbola. Figure 6 illustrates the geometry for this particular optimum capture-escape problem.

The effect of the capture orbit inclination on the minimum total velocity increment is shown in Fig. 7. It is readily apparent that the inclination of the orbit has a significant influence on the velocity increment required to perform the capture and escape maneuvers.

Conclusions

The following observations can be made concerning the work summarized in this paper.

1) The analytical and computational method presented in this paper for determining the optimum orientation for the planetary stopover orbit provides a rapid means for conducting a parametric study of the stopover orbit parameters (a,e,i) for classes of interplanetary missions;

2) The results of such a parametric study used in conjunction with other optimal mission analysis studies can yield information that can result in highly economical mission profiles;

3) The length of time spent in the stopover orbit can be used to advantage, in some cases, in reducing the total velocity increment for the capture and escape maneuvers;

4) The fact that the gradient vector is calculated using a finite differencing technique and provides sufficient accuracy to permit convergence is significant.

References

[1] Cornick, D. E., "A Computational Method for the Determination of the Optimum Parking Orbit Orientation for Planar Capture-Escape Missions," Office Working Paper R-Aero-X-1-68, Aug. 1968, NASA.

[2] Leung, P. T., "An Analytical Model of the Coplanar Planetary Stopover Launch Window Problem with Application to a Venus Mission," TR 387, July 1968, Northrop Nortronics, Huntsville, Ala.

[3] Leung, P. T., "An Analytical Approach to the Orbital Launch Window Problem," Internal Note 62, Oct. 1967, Northrop Nortronics, Huntsville, Ala.

[4] Willis, E. A., Jr., "Optimal Finite-Thrust Transfer Between Planet Approach and Departure Asymptotes with Specified Intermediate Orbit," TN D-4534, 1968, NASA.

[5] Deerwester, J. M., McLaughlin, J. R., and Wolfe, J. F., "Earth-Departure Plane Change and Launch Window Considerations for Interplanetary Missions," *Journal of Spacecraft and Rockets*, Vol. 2, No. 2, Feb. 1966, pp. 169–174.

[6] Young, A. C. and Odom, P. R., "A Computer Simulation of the Orbital Launch Window Problem," AIAA Paper 67-615, Huntsville, Ala., 1967.

[7] Fletcher, R. and Powell, M. J. D., "A Rapidly Convergent Descent Method for Minimization," *The Computer Journal*, Vol. 6, No. 2, July 1963, pp. 163–168.